Adiabatic Waveforms from Extreme-Mass-Ratio Inspirals: An Analytical Approach

Soichiro Isoyama,[1,2] Ryuichi Fujita,[3,4] Alvin J. K. Chua,[5] Hiroyuki Nakano,[6] Adam Pound,[1] and Norichika Sago[7,8]
[1]School of Mathematics and STAG Research Centre, University of Southampton, Southampton SO17 1BJ, United Kingdom
[2]International Institute of Physics, Universidade Federal do Rio Grande do Norte, Campus Universitário, Lagoa Nova, Natal-RN 59078-970, Brazil
[3]Institute of Liberal Arts, Otemon Gakuin University, Osaka 567-8502, Japan
[4]Center for Gravitational Physics, Yukawa Institute for Theoretical Physics, Kyoto University, Kyoto 606-8502, Japan
[5]Theoretical Astrophysics Group, California Institute of Technology, Pasadena, California 91125, USA
[6]Faculty of Law, Ryukoku University, Kyoto 612-8577, Japan
[7]Department of Physics, Kyoto University, Kyoto 606-8502, Japan
[8]Advanced Mathematical Institute, Osaka City University, Osaka 558-8585, Japan

(Received 24 November 2021; accepted 6 May 2022; published 10 June 2022)

Scientific analysis for the gravitational wave detector LISA will require theoretical waveforms from extreme-mass-ratio inspirals (EMRIs) that extensively cover all possible orbital and spin configurations around astrophysical Kerr black holes. However, on-the-fly calculations of these waveforms have not yet overcome the high dimensionality of the parameter space. To confront this challenge, we present a user-ready EMRI waveform model for generic (eccentric and inclined) orbits in Kerr spacetime, using an analytical self-force approach. Our model accurately covers all EMRIs with arbitrary inclination and black hole spin, up to modest eccentricity ($\lesssim 0.3$) and separation ($\gtrsim 2$–10 M from the last stable orbit). In that regime, our waveforms are accurate at the leading "adiabatic" order, and they approximately capture transient self-force resonances that significantly impact the gravitational wave phase. The model fills an urgent need for extensive waveforms in ongoing data-analysis studies, and its individual components will continue to be useful in future science-adequate waveforms.

DOI: 10.1103/PhysRevLett.128.231101

Introduction.—Gravitational wave (GW) astronomy has revealed a cosmos brimming with black holes (BHs) [1–4], and as GW detectors improve, we will continue to learn more about BHs' properties and demographics. In the 2030s, GW detectors in space (LISA, the Laser Interferometer Space Antenna [5], as well as DECIGO [6], TianQin, and Taiji [7–9]) will observe unparalleled probes of BHs: the inspirals of stellar-mass objects into supermassive BHs in galactic cores [10,11]. The waveforms from these extreme-mass-ratio inspirals (EMRIs, with mass ratios $\eta \sim 10^{-4} - 10^{-7}$) will contain a unique wealth of information about the spacetime geometry of BHs, strong-field physics in their vicinity, and the astrophysics of their stellar environments [12–16].

The scientific potential of EMRIs has motivated the community to solve the relativistic two-body problem in the small-mass-ratio regime, making use of gravitational self-force (GSF) theory [17–23]: a perturbative method in which the small body perturbs the central BH's spacetime, and the perturbation drives the body away from geodesic motion. GSF theory has flourished over the past 25 years [24–28], yielding a range of powerful tools for modeling EMRIs [29–36]. The key goal of the EMRI modeling program is to generate waveforms for generic (eccentric and inclined) inspiraling orbits about astrophysical Kerr BHs, accounting for GSF effects. In order to enable accurate extraction of EMRI parameters from a signal, a GSF model must ultimately be accurate to the first subleading (first "postadiabatic") order in η [37–42]. Attaining such accuracy will depend crucially upon calculations at leading order, which can be used to produce "adiabatic" waveforms [43–48] as a baseline in present-day data-analysis studies and for future science-adequate waveforms.

After decades of progress [49–64], adiabatic waveforms for generic Kerr orbits were obtained in 2021 [65]. Still, very few of these (mostly equatorial or spherical orbits) have been simulated so far, and the raw techniques used in that work are unsuitable in the provision of "on the fly" waveforms for data-analysis studies. The main challenge is the high-dimensional parameter space of generic EMRIs. An adiabatic evolution must compute various inputs at fixed points in the parameter space in order to then drive the evolution through it. Populating the vast space sufficiently densely is a very computationally expensive task, and there are ongoing efforts to develop a cost-effective method to ease this burden [63–67].

Meanwhile, there has been significant development of analytical techniques in GSF theory, which invoke a "post-Newtonian" (PN) framework of BH perturbation theory [68,69]. This PN-GSF approach is far less expensive

than numerical GSF calculations, readily covering a large region of parameter space that would be difficult to populate numerically [70–75]. To date, PN-GSF results have informed EMRI waveform modeling indirectly through "effective one-body" [76–80] and "kludge" models [81–87]. Despite being computationally cheap and much desired for LISA studies, the PN-GSF framework has not yet been implemented for relativistic adiabatic waveforms due to its technical complexity.

We here report the first adiabatic EMRI waveform model for generic Kerr orbits based on the analytical PN-GSF approach. Our waveform is a standalone, on-the-fly model within GSF theory, efficiently covering the weak-field region of EMRI parameter space; see Figs. 1 and 2. Among other things, this allows us to consistently account for the transient GSF resonances in the waveform [30,46,88–91]. These resonances will play a crucial role in the detection and measurement of LISA EMRIs, but they have remained out of reach in high-cost relativistic evolutions and have so far only been treated with phenomenological models [92–94].

Furthermore, individual components of our model can be immediately combined with fits to numerical GSF data and environmental effects [95–98] to construct both highly accurate and efficient waveform models [99,100] that will be employed in ongoing LISA preparatory studies (e.g., [101]), as well as in eventual production-level code for LISA's scientific analysis [102]. They can be also used as reference points to inform the development of a universal model of binaries across all mass ratios [103–106]. We expect that our PN-GSF approach will greatly improve the extensiveness and efficiency of EMRI modeling for LISA, in much the same way that analytical relativistic approaches have continued to advance modeling and data-analysis studies for LIGO, Virgo, and KAGRA [107–110].

Below we describe our adiabatic waveforms and assess their domain of validity. Throughout we set $G = c = 1$ and use (t, r, θ, φ) for Boyer-Lindquist coordinates.

Snapshot waveforms from geodesic trajectories.—To set the stage, we first summarize EMRI snapshot waveforms, where the small body's motion is strictly geodesic [54,57,111]. M and a denote the mass and spin parameters of the Kerr BH, $q \equiv a/M$ its dimensionless spin magnitude, and $\mu \ll M$ the mass of the small body (so $\mu/M = \eta$). Our convention is that $q > 0$ ($q < 0$) represents prograde (retrograde) orbits.

A bound Kerr geodesic is confined to a toroidal region given by $r_{\min} \le r \le r_{\max}$ and $\theta_{\min} \le \theta \le \pi - \theta_{\min}$. The orbit is generically triperiodic, uniquely described by three constants of motion $I_A \equiv \{p, e, \iota\}$ [43,112] and three orbital phases $\Phi^A = \{\Phi^r, \Phi^\theta, \Phi^\varphi\}$ with constant frequencies $d\Phi^A/dt = \Omega^A(I_B)$ [113]. The three constant orbital parameters are the *semilatus rectum* $Mp \equiv (2r_{\max}r_{\min})/(r_{\max} + r_{\min})$, orbital eccentricity $e \equiv (r_{\max} - r_{\min})/(r_{\max} + r_{\min})$, and inclination angle $\tan\iota \equiv \sqrt{\hat{C}}/\hat{L}$, where $\hat{L}$ and $\hat{C}$ are the specific azimuthal angular momentum and Carter constant of the geodesic [114]. The orbit's radial, polar, and azimuthal positions are 2π periodic in Φ^r, Φ^θ, and Φ^φ, respectively.

The gravitational radiation from these geodesics can be conveniently computed in the Teukolsky BH perturbation formalism, working with the linear perturbation of the Weyl scalar $\psi_4 = O(\eta)$ [115,116]; at infinity, the two GW polarizations $h_{+,\times}$ are simply given by $\psi_4(r \to \infty) = \frac{1}{2}(\partial^2/\partial t^2)(h_+ - ih_\times)$. ψ_4 in the Fourier domain admits a full separation of variables by means of spin-weighted ($s = -2$) spheroidal harmonics ${}_{-2}S^{a\omega}_{\ell m}(\theta)$. The source geodesic's triperiodicity restricts the perturbation to the discrete frequency spectrum $\omega_{mkn} \equiv m\Omega^\varphi + k\Omega^\theta + n\Omega^r$ for integers m, k, n. We may thus write $h_{+,\times}$ as a multipolar sum of "voices" with those frequencies: $h_+ - ih_\times \propto r^{-1}\sum_{\ell mkn}(Z^\infty_{\ell mkn-2}S^{a\omega_{mkn}}_{\ell m}/\omega^2_{mkn})e^{-i\omega_{mkn}(t-r^*)+im\varphi}$ with $\sum_{\ell mkn} \equiv \sum_{\ell=2}^\infty \sum_{m=-\ell}^\ell \sum_{k=-\infty}^\infty \sum_{n=-\infty}^\infty$ and the Kerr tortoise coordinate r^* [117]. Here, the dimensionless asymptotic amplitudes at infinity $Z^\infty_{\ell mkn}(I_A)$ are obtained by solving the inhomogeneous radial Teukolsky equation mode by mode with a fixed geodesic source, enforcing outgoing (ingoing) boundary conditions at infinity (the horizon). The waveform phase $\omega_{mkn}\cdot(t - r^*)$ is a simple linear combination of the orbital phases $\Phi_{mkn}(t) \equiv m\Phi^\varphi(t) + k\Phi^\theta(t) + n\Phi^r(t)$, evaluated at the retarded time $u = t - r^*$.

Adiabatic waveforms from inspiral trajectories.—We now turn to adiabatic waveforms from orbits that slowly inspiral due to first-order [$O(\eta)$] GSF effects [17,19–21], specifically following the two-timescale framework developed in Refs. [38,39,41]. In this framework, we introduce a "slow time" $\tilde{t} \equiv \eta t$. The trajectory and metric are treated as functions of slowly varying parameters $I_A(\tilde{t}) \equiv \{p(\tilde{t}), e(\tilde{t}), \iota(\tilde{t})\}$ and "fast time" phases Φ^A that evolve with slowly varying frequencies:

$$\frac{d\Phi^A}{dt} = \Omega^A[I_B(\eta t)] \quad \text{or} \quad \frac{d\Phi^A}{d\tilde{t}} = \eta^{-1}\Omega^A[I_B(\tilde{t})], \quad (1)$$

where $\Omega^A(I_B)$ is the same function of I_B as for a geodesic. The dependence on I_A captures the system's evolution on the radiation-reaction timescale $\sim M/\eta$, and the dependence on Φ^A capture the triperiodicity on the orbital timescale $\sim M$.

Adiabatic inspirals and waveforms in this framework can be heuristically understood as a slow-time evolution through the space of geodesic snapshots. The self-forced equations of motion and Teukolsky equations are split into slow- and fast-time equations. At each slow-time step $\tilde{t}$, the leading-order fast-time equations are identical to the equations for a geodesic snapshot, yielding the same Teukolsky amplitudes as a snapshot with the same parameters I_A. The adiabatic waveform can then be written in a

form precisely analogous to the snapshot waveforms described above [41,118],

$$h_+ - ih_\times = -\frac{2\mu}{r}\sum_{\ell mkn}\frac{Z^\infty_{\ell mkn}}{\omega^2_{mkn}}\frac{{}_{-2}S^{a\omega_{mkn}}_{\ell m}}{\sqrt{2\pi}}e^{-i\Phi_{mkn}+im\varphi}, \quad (2)$$

where $Z^\infty_{\ell mkn}$, ω^2_{mkn}, and ${}_{-2}S^{a\omega_{mkn}}_{\ell m}$ are all geodesic functions of I_A, and the snapshot phase $\omega_{mkn}\cdot(t-r^*)$ is now replaced by the adiabatic phase $\Phi_{mkn}(\tilde{u})$ [satisfying Eq. (1)] evaluated at the slow retarded time $\tilde{u}\equiv\eta(t-r^*)$.

The evolution of I_A can be derived from the self-forced equation of motion for the Boyer-Lindquist coordinate trajectory z^μ. If we define "osculating" parameters $I^{\rm osc}_A$ by the condition that $z^\mu(I^{\rm osc}_A,\Phi^A)$ and $dz^\mu/dt(I^{\rm osc}_A,\Phi^A)$ satisfy the geodesic relationships between $\{z^\mu, dz^\mu/dt\}$ and $\{I_A,\Phi^A\}$, then we can straightforwardly derive an equation of the form $dI^{\rm osc}_A/dt = G_A \sim \eta$ [41]. If we write $I^{\rm osc}_A$ and G_A as Fourier series of the form $G_A = \sum_{\mathsf{k}_r\mathsf{k}_\theta} G^{\mathsf{k}_r\mathsf{k}_\theta}_A(I_B)\exp\{i(\mathsf{k}_r\Phi^r+\mathsf{k}_\theta\Phi^\theta)\}$, then at leading order the slowly varying I_A is the stationary, 00 mode of $I^{\rm osc}_A$, and its driving force is the 00 mode of G_A. G^{00}_A involves only the dissipative piece of G_A [30,38,44,46,47], which allows us to express it in terms of the asymptotic flux of radiation [111] in the convenient "flux-balance" form [123–125]

$$\frac{dI_A}{d\tilde{t}} = -M\sum_{\ell mkn}\frac{(\beta_{mkn})_A}{4\pi\omega^3_{mkn}}\{|Z^\infty_{\ell mkn}|^2+\alpha_{\ell mkn}|Z^H_{\ell mkn}|^2\}, \quad (3)$$

where $Z^H_{\ell mkn}(I_A)$ is the Teukolsky amplitude of ψ_4 at the horizon, and $\alpha_{\ell mkn}$ and $(\beta_{mkn})_A$ are certain functions of I_A [71]. The adiabatic evolution is then given by Eqs. (1)–(3).

Transient resonances.—However, the adiabatic-evolution scheme described above has to be altered if, at some instant, $\tilde{t}=\tilde{t}_{\rm res}$, the slowly evolving orbital frequencies, satisfy

$$\omega^{\rm res}(\tilde{t}_{\rm res}) \equiv \beta^r\Omega^r(\tilde{t}_{\rm res}) - \beta^\theta\Omega^\theta(\tilde{t}_{\rm res}) = 0 \quad (4)$$

with a pair of nonzero coprime integers (β^r,β^θ). This condition leads to a transient resonance of GSF effects that occurs for generic EMRIs [30,46,88–91]. At the resonance, otherwise-oscillatory modes of G_A with $\mathsf{k}_r:\mathsf{k}_\theta=\beta^r:-\beta^\theta$ become stationary, and the flux-balance formulas [Eq. (3)] are then enhanced (or diminished) according to [125–131]:

$$\frac{dI^{\rm res}_A}{dt} \equiv \sum\nolimits_{s\neq 0} G^{{\rm res},s}_A e^{is\Phi^{\rm res}}\Big|_{\tilde{t}=\tilde{t}_{\rm res}}. \quad (5)$$

Here, $G^{{\rm res},s}_A \equiv G^{s\beta_r,-s\beta_\theta}_A$ is the sth resonant mode of G_A, and the phase $\Phi^{\rm res}\equiv\beta^r\Phi^r-\beta^\theta\Phi^\theta$ becomes stationary at resonance.

Dissipation drives the orbit through the resonance, with a resonance-crossing time [92,93]

$$\tilde{T}^{{\rm res},s} \equiv \sqrt{\frac{2\pi}{|s\dot{\omega}^{\rm res}|}} \sim M\eta^{-1/2}, \quad (6)$$

where $\dot{\omega}^{\rm res}\equiv d\omega^{\rm res}/d\tilde{t}$ evaluated at the resonance. $\tilde{T}^{{\rm res},s}$ is longer than the orbital timescale $\sim M$, but much shorter than the radiation-reaction timescale $\sim M/\eta$. On the radiation-reaction time, the resonance crossing is effectively instantaneous, and the correction [Eq. (5)] causes a sudden jump $\delta I^{\rm res}_A$ at $\tilde{t}=\tilde{t}_{\rm res}$. Formally expanding the phase $\Phi^{\rm res}(t)$ around the resonance as $\Phi^{\rm res}(t_{\rm res})+\frac{1}{2}\dot{\omega}^{\rm res}(t-t_{\rm res})^2+O(|t-t_{\rm res}|^3)$ with the aid of Eqs. (1) and (4), and integrating Eq. (5) under the stationary phase approximation, we find (see, e.g., Refs. [34,41])

$$\delta I^{\rm res}_A = \sum_{s\neq 0}\tilde{T}^{{\rm res},s}G^{{\rm res},s}_A e^{{\rm sgn}(s\dot{\omega}^{\rm res})\frac{i\pi}{4}+is\Phi^{\rm res}}\Big|_{\tilde{t}=\tilde{t}_{\rm res}} \sim \eta^{1/2}. \quad (7)$$

This induces corresponding abrupt frequency jumps $\delta\Omega^A\sim\eta^{1/2}/M$, resulting in large cumulative phase shifts $\delta\Phi^A\sim\eta^{-1/2}$ a radiation-reaction time after the resonance crossing, which will deteriorate our ability to measure EMRIs.

If we only have access to the leading-order dissipative GSF, we cannot calculate the exact $O(\eta^{1/2})$ jumps for two reasons. First, the size of $\delta I^{\rm res}_A$ in Eq. (7) sensitively depends on the phase $\Phi^{\rm res}$. Calculating the jump therefore requires knowing the phase through first postadiabatic order in the evolution preceding the resonance [132]. Second, the conservative GSF directly contributes to $G^{{\rm res},s}_A$ [125,133]. Accounting for these effects is beyond the current state of the art.

Nevertheless, Eq. (7) correctly determines the jump that is internally consistent with an adiabatic phase evolution. Similarly, discarding the conservative contribution to Eq. (7) yields the correct jump associated with the dissipative GSF. That dissipative piece of $G^{{\rm res},s}_A$ can be constructed directly from the Teukolsky amplitudes as [118]

$$G^{{\rm res},s}_A(I_B) = -M\sum_{\ell mkn}\sum_{\substack{k'=k-s\beta^\theta\\ n'=n+s\beta^r}}\frac{(b_{mkn})_A+k'(c_{mkn})_A}{4\pi\omega^3_{mkn}} \times\{{\rm Re}(Z^\infty_{\ell mkn}\overline{Z^\infty_{\ell mk'n'}})+\alpha_{\ell mkn}{\rm Re}(Z^{\rm H}_{\ell mkn}\overline{Z^{\rm H}_{\ell mk'n'}})\}, \quad (8)$$

where the overline denotes complex conjugation, and $\{(b_{mkn})_A,(c_{mkn})_A\}$ are certain functions of I_A. Because both conservative and dissipative contributions are comparable (at least in a scalar-field toy model [134]), we expect the jumps calculated in this way should qualitatively capture the impact of a resonance crossing at the order-of-magnitude level.

Techniques.—The end-to-end implementation of Eqs. (1), (2), (3), and (7) to generate adiabatic waveforms needs three main inputs across the full parameter space of Kerr spin q and orbital parameters I_A: the frequencies $\Omega^A(I_B)$, the spheroidal harmonics ${}_{-2}S^{a\omega_{mkn}}_{\ell m}$, and the Teukolsky amplitudes $Z^{\infty,\mathrm{H}}_{\ell mkn}$. The expression for $\Omega^A(I_B)$ is given in closed analytical form [113,135]. We can also analytically compute ${}_{-2}S^{a\omega_{mkn}}_{\ell m}$ and $Z^{\infty,\mathrm{H}}_{\ell mkn}$, building on the semianalytical method of solving the Teukolsky equation [136–138] in a small-frequency expansion. This calculation is performed with the analytical module of the Black Hole Perturbation Club (BHPC) code [36] developed in Refs. [70,71,123,139–146]. It assumes the "spheroidicity" $a\omega$, "velocity" $v \equiv \sqrt{1/p}$, and eccentricity e are much smaller than unity but allows arbitrary inclination ι and spin $|q| < 1$ [144]. We obtain ${}_{-2}S^{a\omega_{mkn}}_{\ell m}$ up to $(a\omega_{mkn})^4$ (so $\sim v^{12}$), and $Z^{\infty,H}_{\ell mkn}$ through v^{10} and e^{10} beyond their leading order "Newtonian-circular" terms [147]. This "5PN-e^{10}" calculation includes harmonic modes of $2 \le \ell \le 12$ with $|m| \le \ell$, $|m+k| \le 12$ and $|n| \le 10$, which gives ≈33000 nontrivial modes in total after exploiting mode symmetries [26,54,57,148].

With the analytical inputs in hand, we numerically evolve the system of GW phases [Eq. (1)], polarizations [Eq. (2)], and orbital parameters [Eq. (3)] in the slow time $\tilde{t}$; this numerical evolution (mostly) avoids the 5PN-e^{10} expansion of $\Omega^A(I_B)$, which would severely limit waveform accuracy. The evolution starts with given initial parameters $I_A(0) \equiv I_A(\tilde{t}=0)$ and phases $\Phi^A(0) \equiv \Phi^A(\tilde{t}=0)$ and halts when it satisfies the resonance condition [Eq. (4)], at which time the jump $\delta I^{\mathrm{res}}_A$ is calculated from Eq. (7). We then resume the evolution from $\tilde{t} = \tilde{t}_{\mathrm{res}}$ with the shifted orbital parameters $I_A(\tilde{t}_{\mathrm{res}}) + \delta I^{\mathrm{res}}_A$. These procedures are repeated until the evolution reaches a chosen termination time. The nonresonant part of the evolution is implemented for CPUs, and it is competitive with the numerical kludge code [84], which is the "fastest" (semirelativistic) on-the-fly waveform so far.

Domain of validity.—Before presenting our adiabatic waveform, we compare against an "exact" numerical adiabatic dataset to assess the accuracy of our 5PN-e^{10} Teukolsky amplitudes and fluxes.

In doing so, we also employ the numerical module of the BHPC code [36,53,57,63,149] to compute ${}_{-2}S^{a\omega_{mkn}}_{\ell m}$ for viewing angles $0° \le \theta \le 90°$, and $Z^{\infty,H}_{\ell mkn}$ for $q = \{0, \pm 0.3, \pm 0.5, \pm 0.7, \pm 0.9\}$ and $\iota \sim \{0°, 20°, 40°, 60°, 80°\}$ on a grid in (p, e), where $6 \lesssim p \lesssim 30$ and $0.01 \lesssim e \lesssim 0.4$. The harmonic content of the numerical data is dynamically determined by the condition that the corresponding fluxes $\mathcal{F}^{\mathrm{num}}_A \equiv dI_A/d\tilde{t}$ obtained from Eq. (3) have fractional accuracy $\lesssim 10^{-5}$. We then use two figures of merit for the 5PN-e^{10} analytical results: (i) the "mode-distribution error" of vectorized amplitudes $H \equiv \mathrm{vec}(Z^{\infty}_{\ell mkn} {}_{-2}S^{a\omega_{mkn}}_{\ell m}/\omega^2_{mkn})$ defined by $|1 - \Re(H^{\mathrm{ana}}, H^{\mathrm{num}})/(|H^{\mathrm{ana}}||H^{\mathrm{num}}|)|$, where the inner product $(\cdot,\cdot)$ and its associated norm $|\cdot|$ are (implicitly) Hermitian [64], and (ii) the relative flux error of I_A defined by $|1 - \mathcal{F}^{\mathrm{ana}}_A/\mathcal{F}^{\mathrm{num}}_A|$.

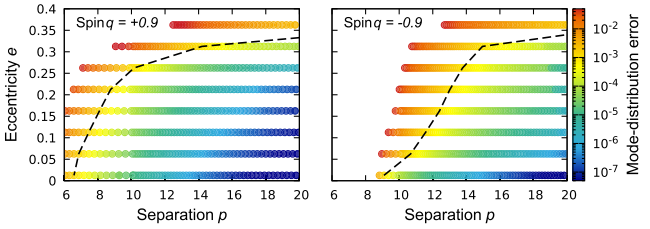

FIG. 1. Mode-distribution error of 5PN-e^{10} amplitudes relative to numerical data. We show the best case of $q = +0.9$, $\iota \approx 80°$ (left) and the worst case of $q = -0.9$, $\iota \approx 20°$ (right); for the latter, the last stable orbit always lies at $p > 8.5$. The dashed curves indicate an error of $\approx 1.0 \times 10^{-3}$, and at $p = 20$ they cross $e \approx 0.33$ ($e \approx 0.35$) in the left (right) panel. The plots are for $(\theta, \varphi) = (45°, 0°)$ but do not depend strongly on the viewing angle because our expansion of ${}_{-2}S^{a\omega_{mkn}}_{\ell m}$ accounts for higher $(a\omega_{mkn})^4$ corrections, valid up to 7 PN.

Figures 1 and 2 show example results of the mode-distribution error and relative flux error, respectively [118]. In addition to the obvious limitation in the small-p (hence large-v) and large-e parameter regions, the errors are also larger with decreasing ι or q when the last stable geodesic orbit lies at $p \gtrsim 6.0$ [150]; the location of this strong-field orbit is difficult to capture with a small-(v, e) expansion. In Fig. 2, we also test Teukolsky-fitted fluxes used in kludge models [81,83,84]. In general, the 5PN-e^{10} fluxes are more accurate than the fitted fluxes for $e \gtrsim 0.2$, independent of q and $\iota \neq 0$.

For parameter inference of LISA-type EMRIs, a mode-distribution error of $\lesssim 1.0 \times 10^{-3}$ is adequate [64,67]. Inference requirements are far more stringent for the fluxes, but these will not be attained even with "exact" adiabatic models. Comparisons to numerical adiabatic evolutions of equatorial orbits [63] suggest that relative flux errors $\lesssim 10^{-2}$ (of $dp/d\tilde{t}$) will suffice for our waveform to maintain phase coherence with adiabatic LISA-EMRI waveforms over several months; this will also be the level of agreement between adiabatic and postadiabatic models [118]. We therefore estimate the domain of validity of the 5PN-e^{10}

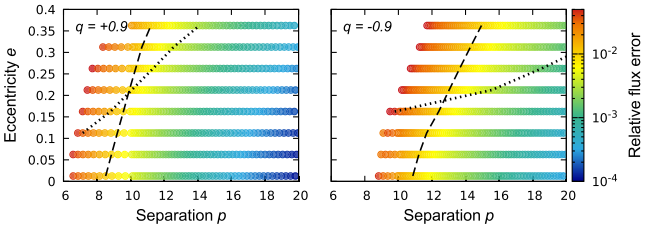

FIG. 2. Error of 5PN-e^{10} fluxes $\mathcal{F}_p (\equiv dp/d\tilde{t})$ relative to numerical flux data, with the same parameters as those in Fig. 1. The dashed curves indicate an error of $\approx 1.0 \times 10^{-2}$, while the dotted curves show, for reference, the same level of error for Teukolsky-fitted fluxes [81,83,84].

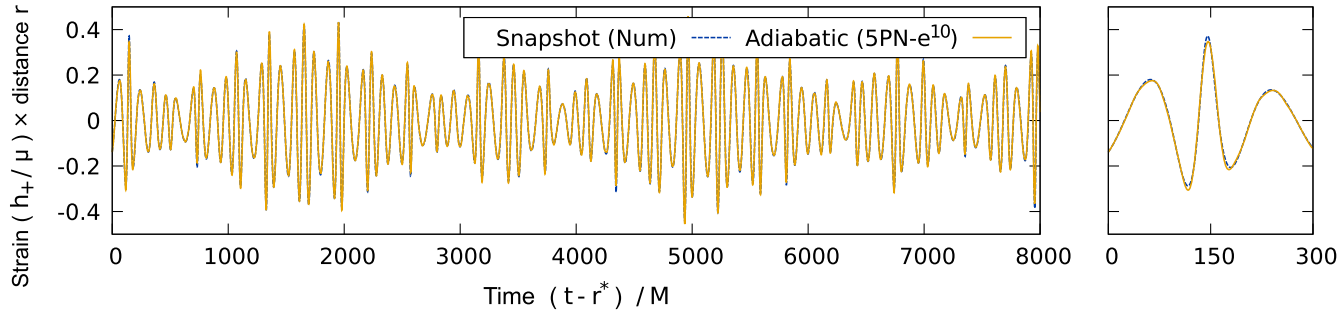

FIG. 3. Left: 5PN-e^{10} adiabatic waveform of a sample EMRI with masses $(M,\mu) = (10^6\,\mathrm{M}_\odot, 10\,\mathrm{M}_\odot)$ and spin $q = 0.9$, starting at $(p_0, e_0, \iota_0) = (9.6, 0.21, 80°)$. We plot the first ≈11 hours ($M \approx 5$ sec) of the evolving waveform at the viewing angle $(\theta, \varphi) = (45°, 0°)$. The rich structure of the waveform is due to the beating of voice sets ω_{mkn}, which encode, for example, periastron precession ($\propto \Omega^\varphi - \Omega^r$) and Lense-Thirring precession ($\propto \Omega^\varphi - \Omega^\theta$). The dashed curve is the reference snapshot waveform from the fixed geodesic orbit with the same initial frequencies and phases at $t = 0$; this was generated using the BHPC's numerical Teukolsky code [57]. Right: the first ≈25 min.

results as $6 \lesssim p \lesssim 20$ and $0 \lesssim e \lesssim 0.3$ across $|q| \leq 0.9$ and $0° \leq \iota \leq 80°$, excluding the parameter region near the last stable orbit.

Sample results.—As a concrete example, we present a 5PN-e^{10} adiabatic waveform with masses and Kerr spin $(\mu, M, q) = (10\mathrm{M}_\odot, 10^6\ \mathrm{M}_\odot, 0.9)$, initial orbital parameters $[p(0), e(0), \iota(0)] = (9.6, 0.21, 80°)$, and initial phases $\Phi^A(0) = 0$. We evolve the EMRI over ≈4 months, starting from the initial apastron $[r(0), \theta(0), \varphi(0)] = \{Mp(0)/[1 - e(0)], \pi/2, 0\}$ with $d\theta(0)/dt < 0$, and ending with final orbital parameter values $(p_\mathrm{f}, e_\mathrm{f}, \iota_\mathrm{f}) \approx (9.23, 0.197, 80.1°)$. During that time the inspiral passes through one strong 3:2 resonance; all other resonances that it encounters are suppressed by additional powers of v and e and contribute negligible jumps according to Eq. (7).

Figure 3 shows the first ≈11 hours of the 5PN-e^{10} adiabatic strain h_+. For reference, we also plot the snapshot strain from the fixed geodesic source (i.e., without GSF effects) with the same initial frequencies, generated by the BHPC's numerical Teukolsky solver [57]; this serves as a benchmark for the 5PN-e^{10} waveform so long as the viewing time is much shorter than the dephasing time $\sim M/(\sqrt{\eta}\Omega^A)$ [34,37], after which the inspiral orbit becomes ∼1 cycle out of phase with the geodesic orbit. The dephasing time of this sample EMRI is ∼2 days. As the figure shows, the 5PN-e^{10} model faithfully approximates the numerical snapshot, a consequence of the small mode distribution error $\approx 5.0 \times 10^{-4}$ in the 5PN-e^{10} amplitudes.

The slow evolution of the adiabatic waveform is more visible in the time-frequency plot [Fig. 4]. The 3:2 resonance occurs at $\tilde{t}_\mathrm{res} \approx 4.3452$ M, where there are abrupt frequency jumps $(\delta\Omega^r/\sqrt{\eta}, \delta\Omega^\theta/\sqrt{\eta}, \delta\Omega^\varphi/\sqrt{\eta}) \approx (4.54 \times 10^{-4}, 1.02 \times 10^{-3}, 1.13 \times 10^{-3})$, corresponding to the jumps $(\delta p^\mathrm{res}/\sqrt{\eta}, \delta e^\mathrm{res}/\sqrt{\eta}, \delta\iota^\mathrm{res}/\sqrt{\eta}) \approx (1.80 \times 10^{-2}, 8.66 \times 10^{-3}, 2.17° \times 10^{-2})$ estimated from Eq. (7). Although the frequency jumps are small ($\propto \sqrt{\eta}$), they lead to large cumulative phase shifts $(\delta\Phi^\mathrm{res}_r, \delta\Phi^\mathrm{res}_\theta, \delta\Phi^\mathrm{res}_\varphi) \approx (2.38, 5.49, 6.13)$ by the termination time $\tilde{t} = 20.0$ M. Such shifts are dramatic compared to LISA's EMRI phase resolution ∼0.1 rad [95,96,151], reconfirming the importance of GSF resonances for EMRI measurements [92–94].

Concluding remarks.—Our PN-GSF adiabatic model represents the first user-ready, relativistic description of EMRI waveforms in the astrophysical scenario of generic Kerr orbits, including an approximate treatment of GSF resonances. It can be used to generate on-the-fly waveforms over the whole weak-field, small-eccentricity region of the EMRI parameter space, with arbitrary orbital inclination

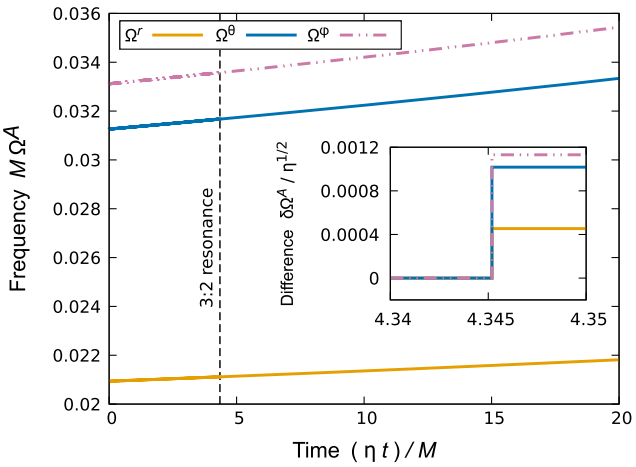

FIG. 4. Slowly evolving orbital frequencies $\Omega^A \equiv \{\Omega^r, \Omega^\theta, \Omega^\varphi\}$ for the sample EMRI waveform in Fig. 3 as a function of the slow time $\tilde{t} = \eta t$. The adiabatic evolution lasts for ≈4months ($\tilde{t} = 20.0$ M). The vertical dashed line marks the 3:2 resonance at $\tilde{t}_\mathrm{res} \approx 4.3452$ M with frequencies $M\Omega^r \approx 2.11 \times 10^{-2}$ and $M\Omega^\theta \approx 3.17 \times 10^{-2}$. The inset enlarges the region near the resonance, showing the difference $\delta\Omega^A := M(\Omega^A_\mathrm{non-res} - \Omega^A_\mathrm{res})$ between the evolution with and without resonance effects. At the resonance, there are order-$\sqrt{\eta}$ discontinuous frequency jumps.

and Kerr spin, thus opening a new front in ongoing EMRI modeling and data analysis efforts [6,101].

In the near term, we will improve our 5PN-e^{10} analytical calculations to cover more of the EMRI parameter space [70,146,152–156]. We will further accelerate our model toward EMRI data analysis, using the efficiency-oriented FASTEMRIWAVEFORMS framework [100], which will enable a highly parallelized implementation with graphics processing units [64,67]. Ultimately, we will work on refining the adiabatic model by combining analytical PN-GSF results with numerical GSF data [26–28,63,65,157–163] to accomplish a science-adequate, postadiabatic waveform for LISA.

Finally, it would be informative to compare our adiabatic evolution with small-mass-ratio results from PN theory [164,165] and fully nonlinear numerical-relativity simulations [166–169]. This may further delineate the applicable region of GSF theory [40,170] for generic binary BHs.

We thank Wataru Hikida and Hideyuki Tagoshi for their direct contributions to an earlier version of this manuscript, Scott A. Hughes for helpful discussions on initial phases and comments on the Supplemental Material, Maarten van de Meent for providing independent numerical data to verify BHPC's Teukolsky results, Leor Barack and Chulmoon Yoo for valuable discussions and comments on the manuscript, and Katsuhiko Ganz, Chris Kavanagh, Koutarou Kyutoku, Yasushi Mino, Takashi Nakamura, Misao Sasaki, Masaru Shibata, and Niels Warburton for very helpful discussions. S. I. is especially grateful to Eric Poisson, Riccardo Sturani, and Takahiro Tanaka for their continuous encouragement and insightful discussion about the (adiabatic) evolution scheme for EMRI dynamics. Finally, we thank all the past and present members of the annual Capra meetings with whom we have discussed the techniques and results presented here (over the past decades). S. I. acknowledges support from STFC through Grant No. ST/R00045X/1, the GWverse COST Action CA16104, "Black holes, gravitational waves and fundamental physic," and the additional financial support of Ministry of Education—MEC during his stay at IIP-Natal-Brazil. A. J. K. C. acknowledges support from the NASA Grants No. 18-LPS18-0027 and 20-LPS20-0005, and from the NSF Grant No. PHY-2011968. A. P. acknowledges the support of a Royal Society University Research Fellowship, Research Grant for Research Fellows, Enhancement Awards, and Exchange Grant. This work was supported in part by JSPS/MEXT KAKENHI Grants No. JP16H02183 (R. F.), JP18H04583 (R. F.), JP21H01082 (R. F., H. N., and N. S.), JP17H06358 (H. N. and N. S.), and JP21K03582 (H. N.).

[1] B. P. Abbott *et al.* (LIGO Scientific, Virgo Collaborations), Phys. Rev. X **9**, 031040 (2019).
[2] R. Abbott *et al.* (LIGO Scientific, Virgo Collaborations), Phys. Rev. X **11**, 021053 (2021).
[3] R. Abbott *et al.*, arXiv:2108.01045.
[4] R. Abbott *et al.*, arXiv:2111.03606.
[5] P. Amaro-Seoane *et al.*, arXiv:1702.00786.
[6] S. Kawamura *et al.*, Prog. Theor. Exp. Phys. **2021**, 05A105 (2021).
[7] J. Mei *et al.* (TianQin Collaboration), Prog. Theor. Exp. Phys. **2021**, 05A107 (2021).
[8] Z. Luo, Y. Wang, Y. Wu, W. Hu, and G. Jin, Prog. Theor. Exp. Phys. **2021**, 05A108 (2021).
[9] Y. Gong, J. Luo, and B. Wang, Nat. Astron. **5**, 881 (2021).
[10] P. Amaro-Seoane, Living Rev. Relativity **21**, 4 (2018).
[11] P. Amaro-Seoane, arXiv:2011.03059.
[12] P. Amaro-Seoane, J. R. Gair, M. Freitag, M. Coleman Miller, I. Mandel, C. J. Cutler, and S. Babak, Classical Quantum Gravity **24**, R113 (2007).
[13] S. Babak, J. Gair, A. Sesana, E. Barausse, C. F. Sopuerta, C. P. L. Berry, E. Berti, P. Amaro-Seoane, A. Petiteau, and A. Klein, Phys. Rev. D **95**, 103012 (2017).
[14] C. Berry, S. Hughes, C. Sopuerta, A. Chua, A. Heffernan, K. Holley-Bockelmann, D. Mihaylov, C. Miller, and A. Sesana, Bull. Am. Astron. Soc. **51**, 42 (2019).
[15] H.-M. Fan, Y.-M. Hu, E. Barausse, A. Sesana, J.-d. Zhang, X. Zhang, T.-G. Zi, and J. Mei, Phys. Rev. D **102**, 063016 (2020).
[16] T.-G. Zi, J.-D. Zhang, H.-M. Fan, X.-T. Zhang, Y.-M. Hu, C. Shi, and J. Mei, Phys. Rev. D **104**, 064008 (2021).
[17] Y. Mino, M. Sasaki, and T. Tanaka, Phys. Rev. D **55**, 3457 (1997).
[18] Y. Mino, M. Sasaki, and T. Tanaka, Prog. Theor. Phys. Suppl. **128**, 373 (1997).
[19] T. C. Quinn and R. M. Wald, Phys. Rev. D **56**, 3381 (1997).
[20] S. E. Gralla and R. M. Wald, Classical Quantum Gravity **25**, 205009 (2008); **28**, 159501(E) (2011).
[21] A. Pound, Phys. Rev. D **81**, 024023 (2010).
[22] A. Pound, Phys. Rev. Lett. **109**, 051101 (2012).
[23] S. E. Gralla, Phys. Rev. D **85**, 124011 (2012).
[24] A. G. Shah, J. L. Friedman, and T. S. Keidl, Phys. Rev. D **86**, 084059 (2012).
[25] M. van de Meent, Phys. Rev. D **94**, 044034 (2016).
[26] M. van de Meent, Phys. Rev. D **97**, 104033 (2018).
[27] A. Pound, B. Wardell, N. Warburton, and J. Miller, Phys. Rev. Lett. **124**, 021101 (2020).
[28] N. Warburton, A. Pound, B. Wardell, J. Miller, and L. Durkan, Phys. Rev. Lett. **127**, 151102 (2021).
[29] Y. Mino, Classical Quantum Gravity **22**, S717 (2005).
[30] T. Tanaka, Prog. Theor. Phys. Suppl. **163**, 120 (2006).
[31] L. Barack, Classical Quantum Gravity **26**, 213001 (2009).
[32] E. Poisson, A. Pound, and I. Vega, Living Rev. Relativity **14**, 7 (2011).
[33] L. Barack *et al.*, Classical Quantum Gravity **36**, 143001 (2019).
[34] L. Barack and A. Pound, Rep. Prog. Phys. **82**, 016904 (2019).
[35] Black Hole Perturbation Toolkit, http://bhptoolkit.org/.
[36] Black Hole Perturbation Club (B. H. P. C.). https://sites.google.com/view/bhpc1996/home.
[37] S. L. Detweiler, Classical Quantum Gravity **22**, S681 (2005).
[38] T. Hinderer and E. E. Flanagan, Phys. Rev. D **78**, 064028 (2008).

[39] J. Miller and A. Pound, Phys. Rev. D **103**, 064048 (2021).
[40] M. van de Meent and H. P. Pfeiffer, Phys. Rev. Lett. **125**, 181101 (2020).
[41] A. Pound and B. Wardell, arXiv:2101.04592.
[42] B. Wardell, A. Pound, N. Warburton, J. Miller, L. Durkan, and A. Le Tiec, arXiv:2112.12265.
[43] S. A. Hughes, Phys. Rev. D **61**, 084004 (2000); **63**, 049902(E) (2001); **65**, 069902(E) (2002); **67**, 089901(E) (2003); **78**, 109902(E) (2008); **90**, 109904(E) (2014).
[44] Y. Mino, Phys. Rev. D **67**, 084027 (2003).
[45] S. A. Hughes, S. Drasco, E. E. Flanagan, and J. Franklin, Phys. Rev. Lett. **94**, 221101 (2005).
[46] Y. Mino, Prog. Theor. Phys. **113**, 733 (2005).
[47] Y. Mino, Prog. Theor. Phys. **115**, 43 (2006).
[48] Y. Mino, Phys. Rev. D **77**, 044008 (2008).
[49] T. Nakamura, K. Oohara, and Y. Kojima, Prog. Theor. Phys. Suppl. **90**, 1 (1987).
[50] L. S. Finn and K. S. Thorne, Phys. Rev. D **62**, 124021 (2000).
[51] K. Glampedakis and D. Kennefick, Phys. Rev. D **66**, 044002 (2002).
[52] S. A. Hughes, Phys. Rev. D **64**, 064004 (2001); **88**, 109902 (E) (2013).
[53] R. Fujita and H. Tagoshi, Prog. Theor. Phys. **112**, 415 (2004).
[54] S. Drasco and S. A. Hughes, Phys. Rev. D **73**, 024027 (2006); **88**, 109905(E) (2013); **90**, 109905(E) (2014).
[55] P. A. Sundararajan, G. Khanna, and S. A. Hughes, Phys. Rev. D **76**, 104005 (2007).
[56] P. A. Sundararajan, G. Khanna, S. A. Hughes, and S. Drasco, Phys. Rev. D **78**, 024022 (2008).
[57] R. Fujita, W. Hikida, and H. Tagoshi, Prog. Theor. Phys. **121**, 843 (2009).
[58] E. Harms, S. Bernuzzi, and B. Brügmann, Classical Quantum Gravity **30**, 115013 (2013).
[59] E. Harms, S. Bernuzzi, A. Nagar, and A. Zenginoglu, Classical Quantum Gravity **31**, 245004 (2014).
[60] S. E. Gralla, S. A. Hughes, and N. Warburton, Classical Quantum Gravity **33**, 155002 (2016); **37**, 109501(E) (2020).
[61] O. Burke, J. R. Gair, and J. Simón, Phys. Rev. D **101**, 064026 (2020).
[62] E. Gourgoulhon, A. Le Tiec, F. H. Vincent, and N. Warburton, Astron. Astrophys. **627**, A92 (2019).
[63] R. Fujita and M. Shibata, Phys. Rev. D **102**, 064005 (2020).
[64] A. J. K. Chua, M. L. Katz, N. Warburton, and S. A. Hughes, Phys. Rev. Lett. **126**, 051102 (2021).
[65] S. A. Hughes, N. Warburton, G. Khanna, A. J. K. Chua, and M. L. Katz, Phys. Rev. D **103**, 104014 (2021).
[66] J. L. Barton, D. J. Lazar, D. J. Kennefick, G. Khanna, and L. M. Burko, Phys. Rev. D **78**, 064042 (2008).
[67] M. L. Katz, A. J. K. Chua, L. Speri, N. Warburton, and S. A. Hughes, Phys. Rev. D **104**, 064047 (2021).
[68] Y. Mino, M. Sasaki, M. Shibata, H. Tagoshi, and T. Tanaka, Prog. Theor. Phys. Suppl. **128**, 1 (1997).
[69] M. Sasaki and H. Tagoshi, Living Rev. Relativity **6**, 6 (2003).
[70] R. Fujita, Prog. Theor. Exp. Phys. **2015**, 33E01 (2015).
[71] N. Sago and R. Fujita, Prog. Theor. Exp. Phys. **2015**, 073E03 (2015).
[72] C. Kavanagh, A. C. Ottewill, and B. Wardell, Phys. Rev. D **93**, 124038 (2016).
[73] D. Bini and A. Geralico, Found. Phys. **48**, 1349 (2018).
[74] D. Bini and A. Geralico, Phys. Rev. D **100**, 104002 (2019).
[75] C. Munna, Ph.D. thesis, North Carolina U., 2020.
[76] N. Yunes, A. Buonanno, S. A. Hughes, M. Coleman Miller, and Y. Pan, Phys. Rev. Lett. **104**, 091102 (2010).
[77] N. Yunes, A. Buonanno, S. A. Hughes, Y. Pan, E. Barausse, M. C. Miller, and W. Throwe, Phys. Rev. D **83**, 044044 (2011); **88**, 109904(E) (2013).
[78] S. Xin, W.-B. Han, and S.-C. Yang, Phys. Rev. D **100**, 084055 (2019).
[79] C. Zhang, W.-B. Han, X.-Y. Zhong, and G. Wang, Phys. Rev. D **104**, 024050 (2021).
[80] S. Albanesi, A. Nagar, and S. Bernuzzi, Phys. Rev. D **104**, 024067 (2021).
[81] K. Glampedakis, S. A. Hughes, and D. Kennefick, Phys. Rev. D **66**, 064005 (2002).
[82] L. Barack and C. Cutler, Phys. Rev. D **69**, 082005 (2004).
[83] J. R. Gair and K. Glampedakis, Phys. Rev. D **73**, 064037 (2006).
[84] S. Babak, H. Fang, J. R. Gair, K. Glampedakis, and S. A. Hughes, Phys. Rev. D **75**, 024005 (2007); **77**, 04990(E) (2008).
[85] C. F. Sopuerta and N. Yunes, Phys. Rev. D **84**, 124060 (2011).
[86] A. J. Chua and J. R. Gair, Classical Quantum Gravity **32**, 232002 (2015).
[87] A. J. K. Chua, C. J. Moore, and J. R. Gair, Phys. Rev. D **96**, 044005 (2017).
[88] T. A. Apostolatos, G. Lukes-Gerakopoulos, and G. Contopoulos, Phys. Rev. Lett. **103**, 111101 (2009).
[89] E. E. Flanagan and T. Hinderer, Phys. Rev. Lett. **109**, 071102 (2012).
[90] J. Brink, M. Geyer, and T. Hinderer, Phys. Rev. Lett. **114**, 081102 (2015).
[91] J. Brink, M. Geyer, and T. Hinderer, Phys. Rev. D **91**, 083001 (2015).
[92] U. Ruangsri and S. A. Hughes, Phys. Rev. D **89**, 084036 (2014).
[93] C. P. L. Berry, R. H. Cole, P. Cañizares, and J. R. Gair, Phys. Rev. D **94**, 124042 (2016).
[94] L. Speri and J. R. Gair, Phys. Rev. D **103**, 124032 (2021).
[95] B. Bonga, H. Yang, and S. A. Hughes, Phys. Rev. Lett. **123**, 101103 (2019).
[96] P. Gupta, B. Bonga, A. J. K. Chua, and T. Tanaka, Phys. Rev. D **104**, 044056 (2021).
[97] A. Coogan, G. Bertone, D. Gaggero, B. J. Kavanagh, and D. A. Nichols, Phys. Rev. D **105**, 043009 (2022).
[98] S. Barsanti, N. Franchini, L. Gualtieri, A. Maselli, and T. P. Sotiriou, arXiv:2203.05003.
[99] EMRI Kludge Suite, https://github.com/alvincjk/EMRI_Kludge_Suite/.
[100] few: Fast EMRI Waveforms, https://bhptoolkit.org/FastEMRIWaveforms/html/index.html.
[101] A. J. K. Chua and C. J. Cutler, arXiv:2109.14254.
[102] LISA Data Challenges, https://lisa-ldc.lal.in2p3.fr/.

[103] Y. Pan, A. Buonanno, R. Fujita, E. Racine, and H. Tagoshi, Phys. Rev. D **83**, 064003 (2011); **87**, 109901(E) (2013).

[104] G. Pratten, S. Husa, C. Garcia-Quiros, M. Colleoni, A. Ramos-Buades, H. Estelles, and R. Jaume, Phys. Rev. D **102**, 064001 (2020).

[105] N. E. M. Rifat, S. E. Field, G. Khanna, and V. Varma, Phys. Rev. D **101**, 081502(R) (2020).

[106] T. Islam, S. E. Field, S. A. Hughes, G. Khanna, V. Varma, M. Giesler, M. A. Scheel, L. E. Kidder, and H. P. Pfeiffer, arXiv:2204.01972.

[107] P. Ajith, S. Babak, Y. Chen, M. Hewitson, B. Krishnan *et al.*, Phys. Rev. D **77**, 104017 (2008); **79**, 129901(E) (2009).

[108] B. Aylott *et al.*, Classical Quantum Gravity **26**, 165008 (2009).

[109] P. Ajith *et al.*, Classical Quantum Gravity **29**, 124001 (2012); **30**, 199401(E) (2013).

[110] I. Hinder *et al.*, Classical Quantum Gravity **31**, 025012 (2014).

[111] N. Sago, T. Tanaka, W. Hikida, and H. Nakano, Prog. Theor. Phys. **114**, 509 (2005).

[112] C. Cutler, D. Kennefick, and E. Poisson, Phys. Rev. D **50**, 3816 (1994).

[113] W. Schmidt, Classical Quantum Gravity **19**, 2743 (2002).

[114] B. Carter, Phys. Rev. **174**, 1559 (1968).

[115] S. Teukolsky, Phys. Rev. Lett. **29**, 1114 (1972).

[116] S. A. Teukolsky, Astrophys. J. **185**, 635 (1973).

[117] S. Teukolsky and W. Press, Astrophys. J. **193**, 443 (1974).

[118] See Supplemental Material at http://link.aps.org/supplemental/10.1103/PhysRevLett.128.231101 (2021) for a comparison with another adiabatic-evolution scheme in Ref. [65]. For a sketch of the derivation of Eq. (8). For additional plots of relative flux errors. Which includes Refs. [119–122], for an estimate of the dephasing between adiabatic and first postadiabatic model.

[119] L. Barack and N. Sago, Phys. Rev. Lett. **102**, 191101 (2009).

[120] A. Le Tiec, E. Barausse, and A. Buonanno, Phys. Rev. Lett. **108**, 131103 (2012).

[121] S. Isoyama, L. Barack, S. R. Dolan, A. Le Tiec, H. Nakano, A. G. Shah, T. Tanaka, and N. Warburton, Phys. Rev. Lett. **113**, 161101 (2014).

[122] M. van de Meent, Phys. Rev. Lett. **118**, 011101 (2017).

[123] N. Sago, T. Tanaka, W. Hikida, K. Ganz, and H. Nakano, Prog. Theor. Phys. **115**, 873 (2006).

[124] S. Drasco, E. E. Flanagan, and S. A. Hughes, Classical Quantum Gravity **22**, S801 (2005).

[125] S. Isoyama, R. Fujita, H. Nakano, N. Sago, and T. Tanaka, Prog. Theor. Exp. Phys. **2019**, 013E01 (2019).

[126] J. Gair, N. Yunes, and C. M. Bender, J. Math. Phys. (N.Y.) **53**, 032503 (2012).

[127] R. Grossman, J. Levin, and G. Perez-Giz, Phys. Rev. D **88**, 023002 (2013).

[128] E. E. Flanagan, S. A. Hughes, and U. Ruangsri, Phys. Rev. D **89**, 084028 (2014).

[129] S. Isoyama, R. Fujita, H. Nakano, N. Sago, and T. Tanaka, Prog. Theor. Exp. Phys. **2013**, 63E01 (2013).

[130] M. van de Meent, Phys. Rev. D **89**, 084033 (2014).

[131] D. P. Mihaylov and J. R. Gair, J. Math. Phys. (N.Y.) **58**, 112501 (2017).

[132] G. Lukes-Gerakopoulos and V. Witzany, Nonlinear effects in emri dynamics and their imprints on gravitational waves, in *Handbook of Gravitational Wave Astronomy*, edited by C. Bambi, S. Katsanevas, and K. D. Kokkotas (Springer Singapore, Singapore, 2020), pp. 1–44.

[133] R. Fujita, S. Isoyama, A. Le Tiec, H. Nakano, N. Sago, and T. Tanaka, Classical Quantum Gravity **34**, 134001 (2017).

[134] Z. Nasipak and C. R. Evans, Phys. Rev. D **104**, 084011 (2021).

[135] R. Fujita and W. Hikida, Classical Quantum Gravity **26**, 135002 (2009).

[136] E. D. Fackerell and R. G. Crossman, J. Math. Phys. (N.Y.) **18**, 1849 (1977).

[137] S. Mano, H. Suzuki, and E. Takasugi, Prog. Theor. Phys. **95**, 1079 (1996).

[138] S. Mano and E. Takasugi, Prog. Theor. Phys. **97**, 213 (1997).

[139] M. Shibata, M. Sasaki, H. Tagoshi, and T. Tanaka, Phys. Rev. D **51**, 1646 (1995).

[140] H. Tagoshi, Prog. Theor. Phys. **93**, 307 (1995); **118**, 577(E) (2007).

[141] H. Tagoshi, M. Shibata, T. Tanaka, and M. Sasaki, Phys. Rev. D **54**, 1439 (1996).

[142] T. Tanaka, H. Tagoshi, and M. Sasaki, Prog. Theor. Phys. **96**, 1087 (1996).

[143] H. Tagoshi, S. Mano, and E. Takasugi, Prog. Theor. Phys. **98**, 829 (1997).

[144] K. Ganz, W. Hikida, H. Nakano, N. Sago, and T. Tanaka, Prog. Theor. Phys. **117**, 1041 (2007).

[145] R. Fujita, Prog. Theor. Phys. **127**, 583 (2012).

[146] R. Fujita, Prog. Theor. Phys. **128**, 971 (2012).

[147] The 5PN-e^{10} results for the spheroidal harmonics ${}_{-2}S^{a\omega}_{\ell m}$, Teukolsky amplitudes $Z^{\infty}_{\ell mkn}$, and fluxes $\mathcal{F}_A$ used in this work are all available for download at https://sites.google.com/view/bhpc1996/data (2021).

[148] Z. Nasipak, T. Osburn, and C. R. Evans, Phys. Rev. D **100**, 064008 (2019).

[149] R. Fujita and H. Tagoshi, Prog. Theor. Phys. **113**, 1165 (2005).

[150] L. C. Stein and N. Warburton, Phys. Rev. D **101**, 064007 (2020).

[151] L. Lindblom, B. J. Owen, and D. A. Brown, Phys. Rev. D **78**, 124020 (2008).

[152] A. G. Shah, Phys. Rev. D **90**, 044025 (2014).

[153] C. Munna and C. R. Evans, Phys. Rev. D **100**, 104060 (2019).

[154] C. Munna, C. R. Evans, S. Hopper, and E. Forseth, Phys. Rev. D **102**, 024047 (2020).

[155] C. Munna, Phys. Rev. D **102**, 124001 (2020).

[156] C. Munna and C. R. Evans, Phys. Rev. D **102**, 104006 (2020).

[157] N. Warburton, S. Akcay, L. Barack, J. R. Gair, and N. Sago, Phys. Rev. D **85**, 061501(R) (2012).

[158] T. Osburn, N. Warburton, and C. R. Evans, Phys. Rev. D **93**, 064024 (2016).

[159] M. Van De Meent and N. Warburton, Classical Quantum Gravity **35**, 144003 (2018).

[160] J. McCart, T. Osburn, and J. Y. J. Burton, Phys. Rev. D **104**, 084050 (2021).

[161] P. Lynch, M. van de Meent, and N. Warburton, arXiv: 2112.05651.
[162] J. Mathews, A. Pound, and B. Wardell, Phys. Rev. D **105**, 084031 (2022).
[163] V. Skoupý and G. Lukes-Gerakopoulos, Phys. Rev. D **105**, 084033 (2022).
[164] C. M. Will and M. Maitra, Phys. Rev. D **95**, 064003 (2017).
[165] A. Tucker and C. M. Will, Phys. Rev. D **104**, 104023 (2021).
[166] A. G. M. Lewis, A. Zimmerman, and H. P. Pfeiffer, Classical Quantum Gravity **34**, 124001 (2017).
[167] M. Fernando, D. Neilsen, H. Lim, E. Hirschmann, and H. Sundar, SIAM J. Sci. Comput. **41**, C97 (2019).
[168] C. O. Lousto and J. Healy, Phys. Rev. Lett. **125**, 191102 (2020).
[169] C. O. Lousto and J. Healy, arXiv:2203.08831.
[170] A. Le Tiec, Int. J. Mod. Phys. D **23**, 1430022 (2014).